

Measurement of the CP -Violating Phase ϕ_s in the Decay $B_s^0 \rightarrow J/\psi\phi$

R. Aaij *et al.*^{*}

(LHCb Collaboration)

(Received 14 December 2011; published 9 March 2012)

We present a measurement of the time-dependent CP -violating asymmetry in $B_s^0 \rightarrow J/\psi\phi$ decays, using data collected with the LHCb detector at the LHC. The decay time distribution of $B_s^0 \rightarrow J/\psi\phi$ is characterized by the decay widths Γ_H and Γ_L of the heavy and light mass eigenstates, respectively, of the $B_s^0 - \bar{B}_s^0$ system and by a CP -violating phase ϕ_s . In a sample of about 8500 $B_s^0 \rightarrow J/\psi\phi$ events isolated from 0.37 fb^{-1} of pp collisions at $\sqrt{s} = 7 \text{ TeV}$, we measure $\phi_s = 0.15 \pm 0.18(\text{stat}) \pm 0.06(\text{syst}) \text{ rad}$. We also find an average B_s^0 decay width $\Gamma_s \equiv (\Gamma_L + \Gamma_H)/2 = 0.657 \pm 0.009(\text{stat}) \pm 0.008(\text{syst}) \text{ ps}^{-1}$ and a decay width difference $\Delta\Gamma_s \equiv \Gamma_L - \Gamma_H = 0.123 \pm 0.029(\text{stat}) \pm 0.011(\text{syst}) \text{ ps}^{-1}$. Our measurement is insensitive to the transformation $(\phi_s, \Delta\Gamma_s) \mapsto (\pi - \phi_s, -\Delta\Gamma_s)$.

DOI: 10.1103/PhysRevLett.108.101803

PACS numbers: 13.25.Hw, 11.30.Er, 12.15.Ff, 12.15.Hh

In the standard model (SM), CP violation arises through a single phase in the Cabibbo-Kobayashi-Maskawa quark mixing matrix [1]. In neutral B meson decays to a final state which is accessible to both B and \bar{B} mesons, the interference between the amplitude for the direct decay and the amplitude for decay after oscillation leads to a time-dependent CP -violating asymmetry between the decay time distributions of B and \bar{B} mesons. The decay $B_s^0 \rightarrow J/\psi\phi$ allows the measurement of such an asymmetry, which can be expressed in terms of the decay width difference of the heavy (H) and light (L) B_s^0 mass eigenstates $\Delta\Gamma_s \equiv \Gamma_L - \Gamma_H$ and a single phase ϕ_s [2]. In the SM, the decay width difference is $\Delta\Gamma_s^{\text{SM}} = 0.087 \pm 0.021 \text{ ps}^{-1}$ [3], while the phase is predicted to be small: $\phi_s^{\text{SM}} = -2 \arg(-V_{ts} V_{tb}^* / V_{cs} V_{cb}^*) = -0.036 \pm 0.002 \text{ rad}$ [4]. This value ignores a possible contribution from subleading decay amplitudes [5]. Contributions from physics beyond the SM could lead to much larger values of ϕ_s [6].

In this Letter, we present measurements of ϕ_s , $\Delta\Gamma_s$, and the average decay width $\Gamma_s \equiv (\Gamma_L + \Gamma_H)/2$. Previous measurements of these quantities have been reported by the CDF and D0 Collaborations [7]. We use an integrated luminosity of 0.37 fb^{-1} of pp collision data recorded at a center-of-mass energy $\sqrt{s} = 7 \text{ TeV}$ by the LHCb experiment during the first half of 2011. The LHCb detector is a forward spectrometer at the Large Hadron Collider and is described in detail in Ref. [8].

We look for $B_s^0 \rightarrow J/\psi\phi$ candidates in decays to $J/\psi \rightarrow \mu^+ \mu^-$ and $\phi \rightarrow K^+ K^-$. Events are selected by a trigger system consisting of a hardware trigger, which selects muon or hadron candidates with high transverse

momentum with respect to the beam direction (p_T), followed by a two-stage software trigger. In the first stage, a simplified event reconstruction is applied. Events are required to have either two well-identified muons with invariant mass above 2.7 GeV or at least one muon or one high- p_T track with a large impact parameter to any primary vertex. In the second stage, a full event reconstruction is performed, and only events with a muon candidate pair with invariant mass within 120 MeV of the nominal J/ψ mass [9] are retained. We adopt units such that $c = 1$ and $\hbar = 1$.

For the final event selection, muon candidates are required to have $p_T > 0.5 \text{ GeV}$. J/ψ candidates are created from pairs of oppositely charged muons that have a common vertex and an invariant mass in the range 3030–3150 MeV. The latter corresponds to about 8 times the $\mu^+ \mu^-$ invariant mass resolution and covers part of the J/ψ radiative tail. The ϕ selection requires two oppositely charged particles that are identified as kaons, form a common vertex, and have an invariant mass within $\pm 12 \text{ MeV}$ of the nominal ϕ mass [9]. The p_T of the ϕ candidate is required to exceed 1 GeV. The mass window covers approximately 90% of the $\phi \rightarrow K^+ K^-$ line shape.

We select B_s^0 candidates from combinations of a J/ψ and a ϕ with invariant mass m_B in the range 5200–5550 MeV. The latter is computed with the invariant mass of the $\mu^+ \mu^-$ pair constrained to the nominal J/ψ mass. The decay time t of the B_s^0 is obtained from a vertex fit that constrains the $B_s^0 \rightarrow \mu^+ \mu^- K^+ K^-$ candidate to originate from the primary vertex [10]. The χ^2 of the fit, which has 7 degrees of freedom, is required to be less than 35. In the small fraction of events with more than one candidate, only the candidate with the smallest χ^2 is kept. B_s^0 candidates are required to have a decay time within the range $0.3 < t < 14.0 \text{ ps}$. Applying a lower bound on the decay time suppresses a large fraction of the prompt combinatorial background while having a small effect on the sensitivity to ϕ_s . From a fit to the m_B

*Full author list given at the end of the article.

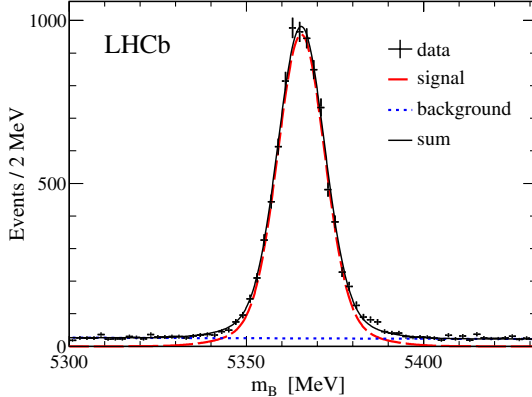


FIG. 1 (color online). Invariant mass distribution for $B_s^0 \rightarrow \mu^+ \mu^- K^+ K^-$ candidates with the mass of the $\mu^+ \mu^-$ pair constrained to the nominal J/ψ mass. Curves for fitted contributions from signal (dashed), background (dotted), and their sum (solid) are overlaid.

distribution, shown in Fig. 1, we extract a signal of 8492 ± 97 events.

The $B_s^0 \rightarrow J/\psi \phi \rightarrow \mu^+ \mu^- K^+ K^-$ decay proceeds via two intermediate spin-1 particles (i.e., with the $K^+ K^-$ pair in a P wave). The final state can be CP -even or CP -odd depending upon the relative orbital angular momentum between the J/ψ and the ϕ . The same final state can also be produced with $K^+ K^-$ pairs with zero relative orbital angular momentum (S -wave) [11]. This S -wave final state is CP -odd. In order to measure ϕ_s , it is necessary to disentangle the CP -even and CP -odd components. This is achieved by analyzing the distribution of the reconstructed decay angles $\Omega = (\theta, \psi, \varphi)$ in the transversity basis [12,13]. In the J/ψ rest frame, we define a right-handed coordinate system such that the x axis is parallel to the direction of the ϕ momentum and the z axis is parallel to the cross-product of the K^- and K^+ momenta. In this frame, θ and φ are the azimuthal and polar angles, respectively, of the μ^+ . The angle ψ is the angle between the K^- momentum and the J/ψ momentum in the rest frame of the ϕ .

We perform an unbinned maximum likelihood fit to the invariant mass m_B , the decay time t , and the three decay angles Ω . The probability density function (PDF) used in the fit consists of signal and background components which include detector resolution and acceptance effects. The PDFs are factorized into separate components for the mass and for the remaining observables.

The signal m_B distribution is described by two Gaussian functions with a common mean. The mean and width of the narrow Gaussian are fit parameters. The fraction of the second Gaussian and its width relative to the narrow Gaussian are fixed to values obtained from simulated events. The m_B distribution for the combinatorial background is described by an exponential function with a slope determined by the fit. Possible peaking background from decays with similar final states such as $B^0 \rightarrow J/\psi K^{*0}$ is found to be negligible from studies using simulated events.

The distribution of the signal decay time and angles is described by a sum of ten terms, corresponding to the four polarization amplitudes and their interference terms. Each of these is the product of a time-dependent function and an angular function [12]

$$\frac{d^4\Gamma(B_s^0 \rightarrow J/\psi \phi)}{dt d\Omega} \propto \sum_{k=1}^{10} h_k(t) f_k(\Omega). \quad (1)$$

The time-dependent functions $h_k(t)$ can be written as

$$h_k(t) = N_k e^{-\Gamma_s t} [c_k \cos(\Delta m_s t) + d_k \sin(\Delta m_s t) + a_k \cosh(\frac{1}{2}\Delta\Gamma_s t) + b_k \sinh(\frac{1}{2}\Delta\Gamma_s t)], \quad (2)$$

where Δm_s is the B_s^0 oscillation frequency. The coefficients N_k and a_k, \dots, d_k can be expressed in terms of ϕ_s and four complex transversity amplitudes A_i at $t = 0$. The label i takes the values $\{\perp, \parallel, 0\}$ for the three P -wave amplitudes and S for the S -wave amplitude. In the fit we parameterize each $A_i(0)$ by its magnitude squared $|A_i(0)|^2$ and its phase δ_i and adopt the convention $\delta_0 = 0$ and $\sum |A_i(0)|^2 = 1$. For a particle produced in a B_s^0 flavor eigenstate, the coefficients in Eq. (2) and the angular functions $f_k(\Omega)$ are then (see [13,14]) given by

k	$f_k(\theta, \psi, \varphi)$	N_k	a_k	b_k	c_k	d_k
1	$2\cos^2\psi(1 - \sin^2\theta\cos^2\phi)$	$ A_0(0) ^2$	1	$-\cos\phi_s$	0	$\sin\phi_s$
2	$\sin^2\psi(1 - \sin^2\theta\sin^2\phi)$	$ A_\parallel(0) ^2$	1	$-\cos\phi_s$	0	$\sin\phi_s$
3	$\sin^2\psi\sin^2\theta$	$ A_\perp(0) ^2$	1	$\cos\phi_s$	0	$-\sin\phi_s$
4	$-\sin^2\psi\sin2\theta\sin\phi$	$ A_\parallel(0)A_\perp(0) $	0	$-\cos(\delta_\perp - \delta_\parallel)\sin\phi_s$	$\sin(\delta_\perp - \delta_\parallel)$	$-\cos(\delta_\perp - \delta_\parallel)\cos\phi_s$
5	$\frac{1}{2}\sqrt{2}\sin2\psi\sin^2\theta\sin2\phi$	$ A_0(0)A_\parallel(0) $	$\cos(\delta_\parallel - \delta_0)$	$-\cos(\delta_\parallel - \delta_0)\cos\phi_s$	0	$\cos(\delta_\parallel - \delta_0)\sin\phi_s$
6	$\frac{1}{2}\sqrt{2}\sin2\psi\sin2\theta\cos\phi$	$ A_0(0)A_\perp(0) $	0	$-\cos(\delta_\perp - \delta_0)\sin\phi_s$	$\sin(\delta_\perp - \delta_0)$	$-\cos(\delta_\perp - \delta_0)\cos\phi_s$
7	$\frac{1}{3}(1 - \sin^2\theta\cos^2\phi)$	$ A_S(0) ^2$	1	$\cos\phi_s$	0	$-\sin\phi_s$
8	$\frac{1}{3}\sqrt{6}\sin\psi\sin^2\theta\sin2\phi$	$ A_S(0)A_\parallel(0) $	0	$-\sin(\delta_\parallel - \delta_S)\sin\phi_s$	$\cos(\delta_\parallel - \delta_S)$	$-\sin(\delta_\parallel - \delta_S)\cos\phi_s$
9	$\frac{1}{3}\sqrt{6}\sin\psi\sin2\theta\cos\phi$	$ A_S(0)A_\perp(0) $	$\sin(\delta_\perp - \delta_S)$	$\sin(\delta_\perp - \delta_S)\cos\phi_s$	0	$-\sin(\delta_\perp - \delta_S)\sin\phi_s$
10	$\frac{4}{3}\sqrt{3}\cos\psi(1 - \sin^2\theta\cos^2\phi)$	$ A_S(0)A_0(0) $	0	$-\sin(\delta_0 - \delta_S)\sin\phi_s$	$\cos(\delta_0 - \delta_S)$	$-\sin(\delta_0 - \delta_S)\cos\phi_s$

We neglect CP violation in mixing and in the decay amplitudes. The differential decay rates for a \bar{B}_s^0 meson produced at time $t = 0$ are obtained by changing the sign of ϕ_s , $A_\perp(0)$, and $A_S(0)$ or, equivalently, the sign of c_k and d_k in the expressions above. The PDF is invariant under the transformation $(\phi_s, \Delta\Gamma_s, \delta_{||}, \delta_\perp, \delta_S) \mapsto (\pi - \phi_s, -\Delta\Gamma_s, -\delta_{||}, \pi - \delta_\perp, -\delta_S)$, which gives rise to a twofold ambiguity in the results.

We have verified that correlations between decay time and decay angles in the background are small enough to be ignored. Using the data in the m_B sidebands, which we define as selected events with m_B outside the range 5311–5411 MeV, we determine that the background decay time distribution can be modeled by a sum of two exponential functions. The lifetime parameters and the relative fraction are determined by the fit. The decay angle distribution is modeled by using a histogram obtained from the data in the m_B sidebands. The normalization of the background with respect to the signal is determined by the fit.

The measurement of ϕ_s requires knowledge of the flavor of the B_s^0 meson at production. We exploit the following flavor-specific features of the accompanying (nonsignal) b -hadron decay to tag the B_s^0 flavor: the charge of a muon or an electron with large transverse momentum produced by semileptonic decays, the charge of a kaon from a subsequent charmed hadron decay, and the momentum-weighted charge of all tracks included in the inclusively reconstructed decay vertex. These signatures are combined by using a neural network to estimate a per-event mistag probability ω , which is calibrated with data from control channels [15]. The fraction of tagged events in the signal sample is $\varepsilon_{\text{tag}} = (24.9 \pm 0.5)\%$. The dilution of the CP asymmetry due to the mistag probability is $D = 1 - 2\omega$. The effective dilution in our signal sample is $D = 0.277 \pm 0.006(\text{stat}) \pm 0.016(\text{syst})$, resulting in an effective tagging efficiency of $\varepsilon_{\text{tag}} D^2 = (1.91 \pm 0.23)\%$. The uncertainty in ω is taken into account by allowing calibration parameters described in Ref. [15] to vary in the fit with Gaussian constraints given by their estimated uncertainties. Both tagged and untagged events are used in the fit. The untagged events dominate the sensitivity to the lifetimes and amplitudes.

To account for the decay time resolution, the PDF is convolved with a sum of three Gaussian functions with a common mean and different widths. Studies on simulated data have shown that selected prompt $J/\psi K^+K^-$ combinations have nearly identical resolution to signal events. Consequently, we determine the parameters of the resolution model from a fit to the decay time distribution of such prompt combinations in the data, after subtracting non- J/ψ events with the sPlot method [16] using the $\mu^+\mu^-$ invariant mass as a discriminating variable. The resulting dilution is equivalent to that of a single Gaussian with a width of 50 fs. The uncertainty on the decay time resolution is estimated to be 4% by varying the selection of

events and by comparing in the simulation the resolutions obtained for prompt combinations and B_s^0 signal events. This uncertainty is accounted for by scaling the widths of the three Gaussians by a common factor of 1.00 ± 0.04 , which is varied in the fit subject to a Gaussian constraint. In a similar fashion, the uncertainty on the mixing frequency is taken into account by varying it within the constraint imposed by the LHCb measurement $\Delta m_s = 17.63 \pm 0.11(\text{stat}) \pm 0.02(\text{syst}) \text{ ps}^{-1}$ [17].

The decay time distribution is affected by two acceptance effects. First, the efficiency decreases approximately linearly with decay time due to inefficiencies in the reconstruction of tracks far from the central axis of the detector. This effect is parameterized as $\epsilon(t) \propto (1 - \beta t)$, where the factor $\beta = 0.016 \text{ ps}^{-1}$ is determined from simulated events. Second, a fraction of approximately 14% of the events has been selected exclusively by a trigger path that exploits large impact parameters of the decay products, leading to a drop in efficiency at small decay times. This effect is described by the empirical acceptance function $\epsilon(t) \propto (at)^c / [1 + (at)^c]$, applied only to these events. The parameters a and c are determined in the fit. As a result, the events selected with impact parameter cuts do effectively not contribute to the measurement of Γ_s .

The uncertainty on the reconstructed decay angles is small and is neglected in the fit. The decay angle acceptance is determined by using simulated events. The deviation from a flat acceptance is due to the LHCb forward geometry and selection requirements on the momenta of final state particles. The acceptance varies by less than 5% over the full range for all three angles.

The results of the fit for the main observables are shown in Table I. The likelihood profile for $\delta_{||}$ is not parabolic, and we therefore quote the 68% confidence level (C.L.) range $3.0 < \delta_{||} < 3.5$. The correlation coefficients for the statistical uncertainties are $\rho(\Gamma_s, \Delta\Gamma_s) = -0.30$, $\rho(\Gamma_s, \phi_s) = 0.12$, and $\rho(\Delta\Gamma_s, \phi_s) = -0.08$. Figure 2 shows the data distribution for decay time and angles with the projections of the best fit PDF overlaid. To assess the overall agreement of the PDF with the data, we calculate the goodness of fit based on the point-to-point dissimilarity test [18]. The p value obtained is 0.68. Figure 3

TABLE I. Fit results for the solution with $\Delta\Gamma_s > 0$ with statistical and systematic uncertainties.

Parameter	Value	σ_{stat}	σ_{syst}
$\Gamma_s [\text{ps}^{-1}]$	0.657	0.009	0.008
$\Delta\Gamma_s [\text{ps}^{-1}]$	0.123	0.029	0.011
$ A_\perp(0) ^2$	0.237	0.015	0.012
$ A_0(0) ^2$	0.497	0.013	0.030
$ A_S(0) ^2$	0.042	0.015	0.018
$\delta_\perp [\text{rad}]$	2.95	0.37	0.12
$\delta_S [\text{rad}]$	2.98	0.36	0.12
$\phi_s [\text{rad}]$	0.15	0.18	0.06

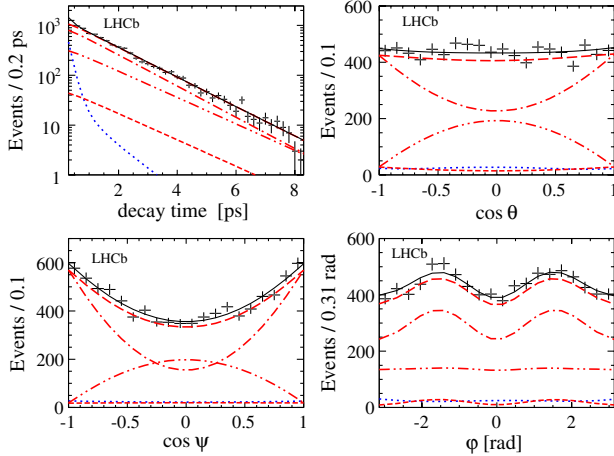


FIG. 2 (color online). Projections for the decay time and transversity angle distributions for events with m_B in a ± 20 MeV range around the B_s^0 mass. The points are the data. The dashed, dotted, and solid lines represent the fitted contributions from signal, background, and their sum, respectively. The remaining curves correspond to different contributions to the signal, namely, the CP -even P -wave (dashed with single dot), the CP -odd P -wave (dashed with double dot), and the S -wave (dashed with triple dot).

shows the 68%, 90%, and 95% C.L. contours in the $\Delta\Gamma_s - \phi_s$ plane. These contours are obtained from the likelihood profile after including systematic uncertainties and correspond to decreases in the natural logarithm of the likelihood, with respect to its maximum, of 1.15, 2.30, and 3.00, respectively.

The sensitivity to ϕ_s stems mainly from its appearance as the amplitude of the $\sin(\Delta m_s t)$ term in Eq. (1), which is diluted by the decay time resolution and mistag probability. Systematic uncertainties from these sources and from the mixing frequency are absorbed in the statistical uncertainties as explained above. Other systematic uncertainties are determined as follows and added in quadrature to give the values shown in Table I.

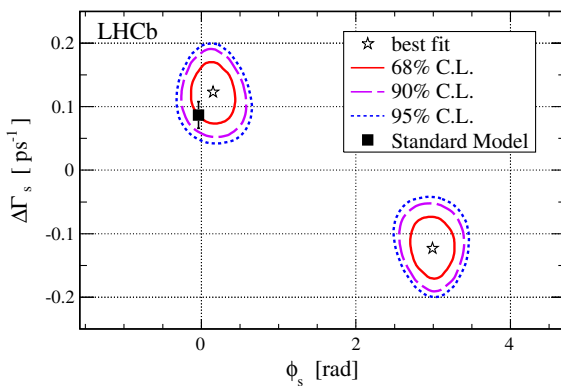


FIG. 3 (color online). Likelihood confidence regions in the $\Delta\Gamma_s - \phi_s$ plane. The black square and error bar correspond to the standard model prediction [3,4].

To test our understanding of the decay angle acceptance, we compare the rapidity and momentum distributions of the kaons and muons of selected B_s^0 candidates in data and simulated events. Only in the kaon momentum distribution do we observe a significant discrepancy. We reweight the simulated events to match the data, rederive the acceptance corrections, and assign the resulting difference in the fit result as a systematic uncertainty. This is the dominant contribution to the systematic uncertainty on all parameters except Γ_s . The limited size of the simulated event sample leads to a small additional uncertainty. The systematic uncertainty due to the background decay angle modeling was found to be negligible by comparing with a fit where the background was removed statistically by using the sPlot method [16].

In the fit, each $|A_i(0)|^2$ is constrained to be greater than zero, while their sum is constrained to unity. This can result in a bias if one or more of the amplitudes is small. This is the case for the S -wave amplitude, which is compatible with zero within 3.2 standard deviations. The resulting biases on the $|A_i(0)|^2$ have been determined by using simulations to be less than 0.010 and are included as systematic uncertainties.

Finally, a systematic uncertainty of 0.008 ps^{-1} was assigned to the measurement of Γ_s due to the uncertainty in the decay time acceptance parameter β . Other systematic uncertainties, such as those from the momentum scale and length scale of the detector, were found to be negligible.

In summary, in a sample of 0.37 fb^{-1} of pp collisions at $\sqrt{s} = 7 \text{ TeV}$ collected with the LHCb detector, we observe $8492 \pm 97 B_s^0 \rightarrow J/\psi K^+ K^-$ events with $K^+ K^-$ invariant mass within ± 12 MeV of the ϕ mass. With these data we perform the most precise measurements of ϕ_s , $\Delta\Gamma_s$, and Γ_s in $B_s^0 \rightarrow J/\psi \phi$ decays, substantially improving upon previous measurements [7] and providing the first direct evidence for a nonzero value of $\Delta\Gamma_s$. Two solutions with equal likelihood are obtained, related by the transformation $(\phi_s, \Delta\Gamma_s) \mapsto (\pi - \phi_s, -\Delta\Gamma_s)$. The solution with positive $\Delta\Gamma_s$ is

$$\begin{aligned}\phi_s &= 0.15 \pm 0.18(\text{stat}) \pm 0.06(\text{syst}) \text{ rad}, \\ \Gamma_s &= 0.657 \pm 0.009(\text{stat}) \pm 0.008(\text{syst}) \text{ ps}^{-1}, \\ \Delta\Gamma_s &= 0.123 \pm 0.029(\text{stat}) \pm 0.011(\text{syst}) \text{ ps}^{-1}\end{aligned}$$

and is in agreement with the standard model prediction [3,4]. Values of ϕ_s in the range $0.52 < \phi_s < 2.62$ and $-2.93 < \phi_s < -0.21$ are excluded at 95% confidence level. In a future publication, we shall differentiate between the two solutions by exploiting the dependence of the phase difference between the P -wave and S -wave contributions on the $K^+ K^-$ invariant mass [14].

We express our gratitude to our colleagues in the CERN accelerator departments for the excellent performance of the LHC. We thank the technical and administrative staff at CERN and at the LHCb institutes and acknowledge support from the National Agencies: CAPES, CNPq,

FAPERJ, and FINEP (Brazil); CERN; NSFC (China); CNRS/IN2P3 (France); BMBF, DFG, HGF, and MPG (Germany); SFI (Ireland); INFN (Italy); FOM and NWO (The Netherlands); SCSR (Poland); ANCS (Romania); MinES of Russia and Rosatom (Russia); MICINN, XuntaGal, and GENCAT (Spain); SNSF and SER (Switzerland); NAS Ukraine (Ukraine); STFC (United Kingdom); NSF (USA). We also acknowledge the support received from the ERC under FP7 and the Region Auvergne.

- [1] M. Kobayashi and T. Maskawa, *Prog. Theor. Phys.* **49**, 652 (1973); N. Cabibbo, *Phys. Rev. Lett.* **10**, 531 (1963).
- [2] A. B. Carter and A. Sanda, *Phys. Rev. Lett.* **45**, 952 (1980); *Phys. Rev. D* **23**, 1567 (1981); I. I. Bigi and A. Sanda, *Nucl. Phys.* **B193**, 85 (1981); **B281**, 41 (1987).
- [3] A. Lenz and U. Nierste, *J. High Energy Phys.* 06 (2007) 072; A. Badin, F. Gabbiani, and A. A. Petrov, *Phys. Lett. B* **653**, 230 (2007); A. Lenz and U. Nierste, arXiv:1102.4274.
- [4] J. Charles *et al.*, *Phys. Rev. D* **84**, 033005 (2011).
- [5] S. Faller, R. Fleischer, and T. Mannel, *Phys. Rev. D* **79**, 014005 (2009).
- [6] For recent overviews, see A. J. Buras, Proc. Sci., EPS-HEP2009 (**2009**) 024; C.-W. Chiang *et al.*, *J. High Energy Phys.* 04 (2010) 031, and references therein.

- [7] T. Aaltonen *et al.* (CDF Collaboration), *Phys. Rev. Lett.* **100**, 161802 (2008); V. Abazov *et al.* (D0 Collaboration), *Phys. Rev. Lett.* **101**, 241801 (2008); V. M. Abazov *et al.* (D0 Collaboration), arXiv:1109.3166; T. Aaltonen *et al.* (CDF Collaboration), arXiv:1112.1726.
- [8] A. A. Alves *et al.* (LHCb Collaboration), *JINST* **3**, S08005 (2008).
- [9] K. Nakamura *et al.* (Particle Data Group), *J. Phys. G* **37**, 075021 (2010).
- [10] W. D. Hulsbergen, *Nucl. Instrum. Methods Phys. Res., Sect. A* **552**, 566 (2005).
- [11] S. Stone and L. Zhang, *Phys. Rev. D* **79**, 074024 (2009).
- [12] A. S. Dighe, I. Dunietz, H. J. Lipkin, and J. L. Rosner, *Phys. Lett. B* **369**, 144 (1996); A. S. Dighe, I. Dunietz, and R. Fleischer, *Eur. Phys. J. C* **6**, 647 (1999).
- [13] I. Dunietz, R. Fleischer, and U. Nierste, *Phys. Rev. D* **63**, 114015 (2001).
- [14] Y. Xie, P. Clarke, G. Cowan, and F. Muheim, *J. High Energy Phys.* **09** (2009) 074.
- [15] R. Aaij *et al.* (LHCb Collaboration), Report No. LHCb-PAPER-2011-027 [Eur. Phys. J. C (to be published)].
- [16] M. Pivk and F. R. Le Diberder, *Nucl. Instrum. Methods Phys. Res., Sect. A* **555**, 356 (2005).
- [17] R. Aaij *et al.* (LHCb Collaboration), arXiv:1112.4311 [Phys. Lett. B (to be published)].
- [18] M. Williams, *JINST* **5**, P09004 (2010).

R. Aaij,²³ C. Abellan Beteta,^{35,a} B. Adeva,³⁶ M. Adinolfi,⁴² C. Adrover,⁶ A. Affolder,⁴⁸ Z. Ajaltouni,⁵ J. Albrecht,³⁷ F. Alessio,³⁷ M. Alexander,⁴⁷ G. Alkhazov,²⁹ P. Alvarez Cartelle,³⁶ A. A. Alves, Jr.,²² S. Amato,² Y. Amhis,³⁸ J. Anderson,³⁹ R. B. Appleby,⁵⁰ O. Aquines Gutierrez,¹⁰ F. Archilli,^{18,37} L. Arrabito,⁵³ A. Artamonov,³⁴ M. Artuso,^{52,37} E. Aslanides,⁶ G. Auriemma,^{22,b} S. Bachmann,¹¹ J. J. Back,⁴⁴ D. S. Bailey,⁵⁰ V. Balagura,^{30,37} W. Baldini,¹⁶ R. J. Barlow,⁵⁰ C. Barschel,³⁷ S. Barsuk,⁷ W. Barter,⁴³ A. Bates,⁴⁷ C. Bauer,¹⁰ Th. Bauer,²³ A. Bay,³⁸ I. Bediaga,¹ S. Belogurov,³⁰ K. Belous,³⁴ I. Belyaev,^{30,37} E. Ben-Haim,⁸ M. Benayoun,⁸ G. Bencivenni,¹⁸ S. Benson,⁴⁶ J. Benton,⁴² R. Bernet,³⁹ M.-O. Bettler,¹⁷ M. van Beuzekom,²³ A. Bien,¹¹ S. Bifani,¹² T. Bird,⁵⁰ A. Bizzeti,^{17,c} P. M. Bjørnstad,⁵⁰ T. Blake,³⁷ F. Blanc,³⁸ C. Blanks,⁴⁹ J. Blouw,¹¹ S. Blusk,⁵² A. Bobrov,³³ V. Bocci,²² A. Bondar,³³ N. Bondar,²⁹ W. Bonivento,¹⁵ S. Borghi,^{47,50} A. Borgia,⁵² T. J. V. Bowcock,⁴⁸ C. Bozzi,¹⁶ T. Brambach,⁹ J. van den Brand,²⁴ J. Bressieux,³⁸ D. Brett,⁵⁰ M. Britsch,¹⁰ T. Britton,⁵² N. H. Brook,⁴² H. Brown,⁴⁸ A. Büchler-Germann,³⁹ I. Burducea,²⁸ A. Bursche,³⁹ J. Buytaert,³⁷ S. Cadeddu,¹⁵ O. Callot,⁷ M. Calvi,^{20,d} M. Calvo Gomez,^{35,a} A. Camboni,³⁵ P. Campana,^{18,37} A. Carbone,¹⁴ G. Carboni,^{21,e} R. Cardinale,^{19,37,f} A. Cardini,¹⁵ L. Carson,⁴⁹ K. Carvalho Akiba,² G. Casse,⁴⁸ M. Cattaneo,³⁷ Ch. Cauet,⁹ M. Charles,⁵¹ Ph. Charpentier,³⁷ N. Chiapolini,³⁹ K. Ciba,³⁷ X. Cid Vidal,³⁶ G. Ciezarek,⁴⁹ P. E. L. Clarke,^{46,37} M. Clemencic,³⁷ H. V. Cliff,⁴³ J. Closier,³⁷ C. Coca,²⁸ V. Coco,²³ J. Cogan,⁶ P. Collins,³⁷ A. Comerma-Montells,³⁵ F. Constantin,²⁸ A. Contu,⁵¹ A. Cook,⁴² M. Coombes,⁴² G. Corti,³⁷ G. A. Cowan,³⁸ R. Currie,⁴⁶ C. D'Ambrosio,³⁷ P. David,⁸ P. N. Y. David,²³ I. De Bonis,⁴ S. De Capua,^{21,e} M. De Cian,³⁹ F. De Lorenzi,¹² J. M. De Miranda,¹ L. De Paula,² P. De Simone,¹⁸ D. Decamp,⁴ M. Deckenhoff,⁹ H. Degaudenzi,^{38,37} L. Del Buono,⁸ C. Deplano,¹⁵ D. Derkach,^{14,37} O. Deschamps,⁵ F. Dettori,²⁴ J. Dickens,⁴³ H. Dijkstra,³⁷ P. Diniz Batista,¹ F. Bonal,^{35,a} S. Domingo Donleavy,⁴⁸ F. Dordei,¹¹ A. Dosil Suárez,³⁶ D. Dossett,⁴⁴ A. Dovbnya,⁴⁰ F. Dupertuis,³⁸ R. Dzhelyadin,³⁴ A. Dziurda,²⁵ S. Easo,⁴⁵ U. Egede,⁴⁹ V. Egorychev,³⁰ S. Eidelman,³³ D. van Eijk,²³ F. Eisele,¹¹ S. Eisenhardt,⁴⁶ R. Ekelhof,⁹ L. Eklund,⁴⁷ Ch. Elsasser,³⁹ D. Elsby,⁵⁵ D. Esperante Pereira,³⁶ L. Estève,⁴³ A. Falabella,^{16,14,g} E. Fanchini,^{20,d} C. Färber,¹¹ G. Fardell,⁴⁶ C. Farinelli,²³ S. Farry,¹² V. Fave,³⁸ V. Fernandez Albor,³⁶ M. Ferro-Luzzi,³⁷ S. Filippov,³² C. Fitzpatrick,⁴⁶ M. Fontana,¹⁰ F. Fontanelli,^{19,f} R. Forty,³⁷ M. Frank,³⁷ C. Frei,³⁷ M. Frosini,^{17,37,h} S. Furcas,²⁰ A. Gallas Torreira,³⁶ D. Galli,^{14,i} M. Gandelman,² P. Gandini,⁵¹ Y. Gao,³ J.-C. Garnier,³⁷ J. Garofoli,⁵² J. Garra Tico,⁴³ L. Garrido,³⁵ D. Gascon,³⁵ C. Gaspar,³⁷ N. Gauvin,³⁸ M. Gersabeck,³⁷ T. Gershon,^{44,37} Ph. Ghez,⁴ V. Gibson,⁴³ V. V. Gligorov,³⁷

- C. Göbel,⁵⁴ D. Golubkov,³⁰ A. Golutvin,^{49,30,37} A. Gomes,² H. Gordon,⁵¹ M. Grabalosa Gándara,³⁵
 R. Graciani Diaz,³⁵ L. A. Granado Cardoso,³⁷ E. Graugés,³⁵ G. Graziani,¹⁷ A. Grecu,²⁸ E. Greening,⁵¹ S. Gregson,⁴³
 B. Gui,⁵² E. Gushchin,³² Yu. Guz,³⁴ T. Gys,³⁷ G. Haefeli,³⁸ C. Haen,³⁷ S. C. Haines,⁴³ T. Hampson,⁴²
 S. Hansmann-Menzemer,¹¹ R. Harji,⁴⁹ N. Harnew,⁵¹ J. Harrison,⁵⁰ P. F. Harrison,⁴⁴ T. Hartmann,⁵⁶ J. He,⁷
 V. Heijne,²³ K. Hennessy,⁴⁸ P. Henrard,⁵ J. A. Hernando Morata,³⁶ E. van Herwijnen,³⁷ E. Hicks,⁴⁸ K. Holubyev,¹¹
 P. Hopchev,⁴ W. Hulsbergen,²³ P. Hunt,⁵¹ T. Huse,⁴⁸ R. S. Huston,¹² D. Hutchcroft,⁴⁸ D. Hynds,⁴⁷ V. Iakovenko,⁴¹
 P. Ilten,¹² J. Imong,⁴² R. Jacobsson,³⁷ A. Jaeger,¹¹ M. Jahjah Hussein,⁵ E. Jans,²³ F. Jansen,²³ P. Jaton,³⁸
 B. Jean-Marie,⁷ F. Jing,³ M. John,⁵¹ D. Johnson,⁵¹ C. R. Jones,⁴³ B. Jost,³⁷ M. Kaballo,⁹ S. Kandybei,⁴⁰
 M. Karacson,³⁷ T. M. Karbach,⁹ J. Keaveney,¹² I. R. Kenyon,⁵⁵ U. Kerzel,³⁷ T. Ketel,²⁴ A. Keune,³⁸ B. Khanji,⁶
 Y. M. Kim,⁴⁶ M. Knecht,³⁸ P. Koppenburg,²³ A. Kozlinskiy,²³ L. Kravchuk,³² K. Kreplin,¹¹ M. Kreps,⁴⁴
 G. Krocker,¹¹ P. Krokovny,¹¹ F. Kruse,⁹ K. Kruzelecki,³⁷ M. Kucharczyk,^{20,25,37,d} T. Kvaratskheliya,^{30,37}
 V. N. La Thi,³⁸ D. Lacarrere,³⁷ G. Lafferty,⁵⁰ A. Lai,¹⁵ D. Lambert,⁴⁶ R. W. Lambert,²⁴ E. Lanciotti,³⁷
 G. Lanfranchi,¹⁸ C. Langenbruch,¹¹ T. Latham,⁴⁴ C. Lazzeroni,⁵⁵ R. Le Gac,⁶ J. van Leerdam,²³ J.-P. Lees,⁴
 R. Lefèvre,⁵ A. Leflat,^{31,37} J. Lefrançois,⁷ O. Leroy,⁶ T. Lesiak,²⁵ L. Li,³ L. Li Gioi,⁵ M. Lieng,⁹ M. Liles,⁴⁸
 R. Lindner,³⁷ C. Linn,¹¹ B. Liu,³ G. Liu,³⁷ J. von Loeben,²⁰ J. H. Lopes,² E. Lopez Asamar,³⁵ N. Lopez-March,³⁸
 H. Lu,^{38,3} J. Luisier,³⁸ A. Mac Raighne,⁴⁷ F. Machefert,⁷ I. V. Machikhiliyan,^{4,30} F. Maciuc,¹⁰ O. Maev,^{29,37}
 J. Magnin,¹ S. Malde,⁵¹ R. M. D. Mamunur,³⁷ G. Manca,^{15,j} G. Mancinelli,⁶ N. Mangiafave,⁴³ U. Marconi,¹⁴
 R. Märki,³⁸ J. Marks,¹¹ G. Martellotti,²² A. Martens,⁸ L. Martin,⁵¹ A. Martín Sánchez,⁷ D. Martinez Santos,³⁷
 A. Massafferri,¹ Z. Mathe,¹² C. Matteuzzi,²⁰ M. Matveev,²⁹ E. Maurice,⁶ B. Maynard,⁵² A. Mazurov,^{16,32,37}
 G. McGregor,⁵⁰ R. McNulty,¹² M. Meissner,¹¹ M. Merk,²³ J. Merkel,⁹ R. Messi,^{21,e} S. Miglioranzi,³⁷
 D. A. Milanes,^{13,37} M.-N. Minard,⁴ J. Molina Rodriguez,⁵⁴ S. Monteil,⁵ D. Moran,¹² P. Morawski,²⁵ R. Mountain,⁵²
 I. Mous,²³ F. Muheim,⁴⁶ K. Müller,³⁹ R. Muresan,^{28,38} B. Muryn,²⁶ B. Muster,³⁸ M. Musy,³⁵ J. Mylroie-Smith,⁴⁸
 P. Naik,⁴² T. Nakada,³⁸ R. Nandakumar,⁴⁵ I. Nasteva,¹ M. Nedos,⁹ M. Needham,⁴⁶ N. Neufeld,³⁷ C. Nguyen-Mau,^{38,k}
 M. Nicol,⁷ V. Niess,⁵ N. Nikitin,³¹ A. Nomerotski,⁵¹ A. Novoselov,³⁴ A. Oblakowska-Mucha,²⁶ V. Obraztsov,³⁴
 S. Oggero,²³ S. Ogilvy,⁴⁷ O. Okhrimenko,⁴¹ R. Oldeman,^{15,j} M. Orlandea,²⁸ J. M. Otalora Goicochea,² P. Owen,⁴⁹
 K. Pal,⁵² J. Palacios,³⁹ A. Palano,^{13,l} M. Palutan,¹⁸ J. Panman,³⁷ A. Papanestis,⁴⁵ M. Pappagallo,⁴⁷ C. Parkes,^{50,37}
 C. J. Parkinson,⁴⁹ G. Passaleva,¹⁷ G. D. Patel,⁴⁸ M. Patel,⁴⁹ S. K. Paterson,⁴⁹ G. N. Patrick,⁴⁵ C. Patrignani,^{19,f}
 C. Pavel-Nicorescu,²⁸ A. Pazos Alvarez,³⁶ A. Pellegrino,²³ G. Penso,^{22,m} M. Pepe Altarelli,³⁷ S. Perazzini,^{14,i}
 D. L. Perego,^{20,d} E. Perez Trigo,³⁶ A. Pérez-Calero Yzquierdo,³⁵ P. Perret,⁵ M. Perrin-Terrin,⁶ G. Pessina,²⁰
 A. Petrella,^{16,37} A. Petrolini,^{19,f} A. Phan,⁵² E. Picatoste Olloqui,³⁵ B. Pie Valls,³⁵ B. Pietrzyk,⁴ T. Pilar,⁴⁴ D. Pinci,²²
 R. Plackett,⁴⁷ S. Playfer,⁴⁶ M. Plo Casasus,³⁶ G. Polok,²⁵ A. Poluektov,^{44,33} E. Polycarpo,² D. Popov,¹⁰ B. Popovici,²⁸
 C. Potterat,³⁵ A. Powell,⁵¹ J. Prisciandaro,³⁸ V. Pugatch,⁴¹ A. Puig Navarro,³⁵ W. Qian,⁵² J. H. Rademacker,⁴²
 B. Rakotomiaramanana,³⁸ M. S. Rangel,² I. Raniuk,⁴⁰ G. Raven,²⁴ S. Redford,⁵¹ M. M. Reid,⁴⁴ A. C. dos Reis,¹
 S. Ricciardi,⁴⁵ K. Rinnert,⁴⁸ D. A. Roa Romero,⁵ P. Robbe,⁷ E. Rodrigues,^{47,50} F. Rodriguez,² P. Rodriguez Perez,³⁶
 G. J. Rogers,⁴³ S. Roiser,³⁷ V. Romanovsky,³⁴ M. Rosello,^{35,a} J. Rouvinet,³⁸ T. Ruf,³⁷ H. Ruiz,³⁵ G. Sabatino,^{21,e}
 J. J. Saborido Silva,³⁶ N. Sagidova,²⁹ P. Sail,⁴⁷ B. Saitta,^{15,j} C. Salzmann,³⁹ M. Sannino,^{19,f} R. Santacesaria,²²
 C. Santamarina Rios,³⁶ R. Santinelli,³⁷ E. Santovetti,^{21,e} M. Sapunov,⁶ A. Sarti,^{18,m} C. Satriano,^{22,b} A. Satta,²¹
 M. Savrie,^{16,g} D. Savrina,³⁰ P. Schaack,⁴⁹ M. Schiller,²⁴ S. Schleich,⁹ M. Schlupp,⁹ M. Schmelling,¹⁰ B. Schmidt,³⁷
 O. Schneider,³⁸ A. Schopper,³⁷ M.-H. Schune,⁷ R. Schwemmer,³⁷ B. Sciascia,¹⁸ A. Sciubba,^{18,m} M. Seco,³⁶
 A. Semennikov,³⁰ K. Senderowska,²⁶ I. Sepp,⁴⁹ N. Serra,³⁹ J. Serrano,⁶ P. Seyfert,¹¹ M. Shapkin,³⁴ I. Shapoval,^{40,37}
 P. Shatalov,³⁰ Y. Shcheglov,²⁹ T. Shears,⁴⁸ L. Shekhtman,³³ O. Shevchenko,⁴⁰ V. Shevchenko,³⁰ A. Shires,⁴⁹
 R. Silva Coutinho,⁴⁴ T. Skwarnicki,⁵² A. C. Smith,³⁷ N. A. Smith,⁴⁸ E. Smith,^{51,45} K. Sobczak,⁵ F. J. P. Soler,⁴⁷
 A. Solomin,⁴² F. Soomro,¹⁸ B. Souza De Paula,² B. Spaan,⁹ A. Sparkes,⁴⁶ P. Spradlin,⁴⁷ F. Stagni,³⁷ S. Stahl,¹¹
 O. Steinkamp,³⁹ S. Stoica,²⁸ S. Stone,^{52,37} B. Storaci,²³ M. Straticiu,²⁸ U. Straumann,³⁹ V. K. Subbiah,³⁷
 S. Swientek,⁹ M. Szczekowski,²⁷ P. Szczypka,³⁸ T. Szumlak,²⁶ S. T'Jampens,⁴ E. Teodorescu,²⁸ F. Teubert,³⁷
 C. Thomas,⁵¹ E. Thomas,³⁷ J. van Tilburg,¹¹ V. Tisserand,⁴ M. Tobin,³⁹ S. Topp-Joergensen,⁵¹ N. Torr,⁵¹
 E. Tournefier,^{4,49} M. T. Tran,³⁸ A. Tsaregorodtsev,⁶ N. Tuning,²³ M. Ubeda Garcia,³⁷ A. Ukleja,²⁷ P. Urquijo,⁵²
 U. Uwer,¹¹ V. Vagnoni,¹⁴ G. Valenti,¹⁴ R. Vazquez Gomez,³⁵ P. Vazquez Regueiro,³⁶ S. Vecchi,¹⁶ J. J. Velthuis,⁴²
 M. Veltri,^{17,n} B. Viaud,⁷ I. Videau,⁷ X. Vilasis-Cardona,^{35,a} J. Visniakov,³⁶ A. Vollhardt,³⁹ D. Volyanskyy,¹⁰
 D. Voong,⁴² A. Vorobyev,²⁹ H. Voss,¹⁰ S. Wandernoth,¹¹ J. Wang,⁵² D. R. Ward,⁴³ N. K. Watson,⁵⁵ A. D. Webber,⁵⁰
 D. Websdale,⁴⁹ M. Whitehead,⁴⁴ D. Wiedner,¹¹ L. Wiggers,²³ G. Wilkinson,⁵¹ M. P. Williams,^{44,45} M. Williams,⁴⁹

F. F. Wilson,⁴⁵ J. Wishahi,⁹ M. Witek,²⁵ W. Witzeling,³⁷ S. A. Wotton,⁴³ K. Wyllie,³⁷ Y. Xie,⁴⁶ F. Xing,⁵¹ Z. Xing,⁵² Z. Yang,³ R. Young,⁴⁶ O. Yushchenko,³⁴ M. Zavertyaev,^{10,o} F. Zhang,³ L. Zhang,⁵² W. C. Zhang,¹² Y. Zhang,³ A. Zhelezov,¹¹ L. Zhong,³ E. Zverev,³¹ and A. Zvyagin³⁷

(LHCb Collaboration)

¹*Centro Brasileiro de Pesquisas Físicas (CBPF), Rio de Janeiro, Brazil*

²*Universidade Federal do Rio de Janeiro (UFRJ), Rio de Janeiro, Brazil*

³*Center for High Energy Physics, Tsinghua University, Beijing, China*

⁴*LAPP, Université de Savoie, CNRS/IN2P3, Annecy-Le-Vieux, France*

⁵*Clermont Université, Université Blaise Pascal, CNRS/IN2P3, LPC, Clermont-Ferrand, France*

⁶*CPPM, Aix-Marseille Université, CNRS/IN2P3, Marseille, France*

⁷*LAL, Université Paris-Sud, CNRS/IN2P3, Orsay, France*

⁸*LPNHE, Université Pierre et Marie Curie, Université Paris Diderot, CNRS/IN2P3, Paris, France*

⁹*Fakultät Physik, Technische Universität Dortmund, Dortmund, Germany*

¹⁰*Max-Planck-Institut für Kernphysik (MPIK), Heidelberg, Germany*

¹¹*Physikalisches Institut, Ruprecht-Karls-Universität Heidelberg, Heidelberg, Germany*

¹²*School of Physics, University College Dublin, Dublin, Ireland*

¹³*Sezione INFN di Bari, Bari, Italy*

¹⁴*Sezione INFN di Bologna, Bologna, Italy*

¹⁵*Sezione INFN di Cagliari, Cagliari, Italy*

¹⁶*Sezione INFN di Ferrara, Ferrara, Italy*

¹⁷*Sezione INFN di Firenze, Firenze, Italy*

¹⁸*Laboratori Nazionali dell'INFN di Frascati, Frascati, Italy*

¹⁹*Sezione INFN di Genova, Genova, Italy*

²⁰*Sezione INFN di Milano Bicocca, Milano, Italy*

²¹*Sezione INFN di Roma Tor Vergata, Roma, Italy*

²²*Sezione INFN di Roma La Sapienza, Roma, Italy*

²³*Nikhef National Institute for Subatomic Physics, Amsterdam, The Netherlands*

²⁴*Nikhef National Institute for Subatomic Physics and Vrije Universiteit, Amsterdam, The Netherlands*

²⁵*Henryk Niewodniczanski Institute of Nuclear Physics Polish Academy of Sciences, Kraców, Poland*

²⁶*AGH University of Science and Technology, Kraców, Poland*

²⁷*Soltan Institute for Nuclear Studies, Warsaw, Poland*

²⁸*Horia Hulubei National Institute of Physics and Nuclear Engineering, Bucharest-Magurele, Romania*

²⁹*Petersburg Nuclear Physics Institute (PNPI), Gatchina, Russia*

³⁰*Institute of Theoretical and Experimental Physics (ITEP), Moscow, Russia*

³¹*Institute of Nuclear Physics, Moscow State University (SINP MSU), Moscow, Russia*

³²*Institute for Nuclear Research of the Russian Academy of Sciences (INR RAN), Moscow, Russia*

³³*Budker Institute of Nuclear Physics (SB RAS) and Novosibirsk State University, Novosibirsk, Russia*

³⁴*Institute for High Energy Physics (IHEP), Protvino, Russia*

³⁵*Universitat de Barcelona, Barcelona, Spain*

³⁶*Universidad de Santiago de Compostela, Santiago de Compostela, Spain*

³⁷*European Organization for Nuclear Research (CERN), Geneva, Switzerland*

³⁸*Ecole Polytechnique Fédérale de Lausanne (EPFL), Lausanne, Switzerland*

³⁹*Physik-Institut, Universität Zürich, Zürich, Switzerland*

⁴⁰*NSC Kharkiv Institute of Physics and Technology (NSC KIPT), Kharkiv, Ukraine*

⁴¹*Institute for Nuclear Research of the National Academy of Sciences (KINR), Kyiv, Ukraine*

⁴²*H. H. Wills Physics Laboratory, University of Bristol, Bristol, United Kingdom*

⁴³*Cavendish Laboratory, University of Cambridge, Cambridge, United Kingdom*

⁴⁴*Department of Physics, University of Warwick, Coventry, United Kingdom*

⁴⁵*STFC Rutherford Appleton Laboratory, Didcot, United Kingdom*

⁴⁶*School of Physics and Astronomy, University of Edinburgh, Edinburgh, United Kingdom*

⁴⁷*School of Physics and Astronomy, University of Glasgow, Glasgow, United Kingdom*

⁴⁸*Oliver Lodge Laboratory, University of Liverpool, Liverpool, United Kingdom*

⁴⁹*Imperial College London, London, United Kingdom*

⁵⁰*School of Physics and Astronomy, University of Manchester, Manchester, United Kingdom*

⁵¹*Department of Physics, University of Oxford, Oxford, United Kingdom*

⁵²*Syracuse University, Syracuse, New York, USA*

⁵³*CC-IN2P3, CNRS/IN2P3, Lyon-Villeurbanne, France, associated member*

⁵⁴*Pontifícia Universidade Católica do Rio de Janeiro (PUC-Rio), Rio de Janeiro, Brazil*⁵⁵*University of Birmingham, Birmingham, United Kingdom*⁵⁶*Physikalisches Institut, Universität Rostock, Rostock, Germany*^aAlso at LIFAELS, La Salle, Universitat Ramon Llull, Barcelona, Spain.^bAlso at Università della Basilicata, Potenza, Italy.^cAlso at Università di Modena e Reggio Emilia, Modena, Italy.^dAlso at Università di Milano Bicocca, Milano, Italy.^eAlso at Università di Roma Tor Vergata, Roma, Italy.^fAlso at Università di Genova, Genova, Italy.^gAlso at Università di Ferrara, Ferrara, Italy.^hAlso at Università di Firenze, Firenze, Italy.ⁱAlso at Università di Bologna, Bologna, Italy.^jAlso at Università di Cagliari, Cagliari, Italy.^kAlso at Hanoi University of Science, Hanoi, Viet Nam.^lAlso at Università di Bari, Bari, Italy.^mAlso at Università di Roma La Sapienza, Roma, Italy.ⁿAlso at Università di Urbino, Urbino, Italy.^oAlso at P.N. Lebedev Physical Institute, Russian Academy of Science (LPI RAS), Moscow, Russia.